Supporting Information for:

Dynamic Control of Nano-Cavities with Tunable Metal Oxides

Jongbum Kim[1,4], Enrico G. Carnemolla[2], Clayton DeVault[3], Amr M. Shalout[1], Daniele Faccio[2], Vladimir M. Shalaev[1], Alexander V. Kildishev[1], Marcello Ferrera[2] and Alexandra Boltasseva[1]

[1] School of Electrical and Computer Engineering, Purdue University and Birck Nanotechnology Center, West Lafayette, IN 47907, USA

[2] Institute of Photonics and Quantum Sciences, Heriot-Watt University, SUPA, Edinburg, Scotland, EH14 4As, UK

[3] Dept. of Physics & Astronomy and Birck Nanotechnology Center, Purdue University, West Lafayette, 47909, USA

[4] Institute for Research in Electronics and Applied Physics, University of Maryland, College Park, Maryland 20742, USA

E-mail: aeb@purdue.edu

1. Fabrication of Nano-Cavities

The designed structures are compatible with nanofabrication techniques. The fabrication process flow is depicted in Fig. S1. The label of each geometry is matched with the sketched samples in Fig. 1.b. As shown in Fig. S1, we deposited 25 nm-thick Ag film and 25 nm-thick Al_2O_3 film on 4 glass substrates by electron beam evaporator. For the fabrication of active nano-cavities (i.e. inclusive of the G:ZnO layer), a 70 nm-thick Ga:ZnO film is deposited on two of the samples by pulsed laser deposition (PVD Products, Inc.). By using e-beam lithography (Vistec VB6), Ag nano-structures were patterned on two samples followed by lift-off process. On top of the patterned resist, 30 nm-thick Ag film was deposited with a 2 nm-thick germanium layer used to

improve adhesion, and the sample was dipped in ZDMAC (dimethylacetamide) for 20 minutes. For planar surface of spacer layer on top of Ag metasurface, we deposited 800 nm-thick Al_2O_3 film on top of Ag metasurface and etched it down to desired thickness (205nm) by reactive ion etching process (Panasonic E620 etcher). The roughness of etched PMMA spacer on top of metasurface is around 2nm. Finally, 24nm thick Ag film for top mirror layer and 30nm thick alumina layer for protection of Ag were deposited on top of PMMA spacer. All samples were prepared at the same time to unify the surface condition and thickness for individual component in nano-cavities.

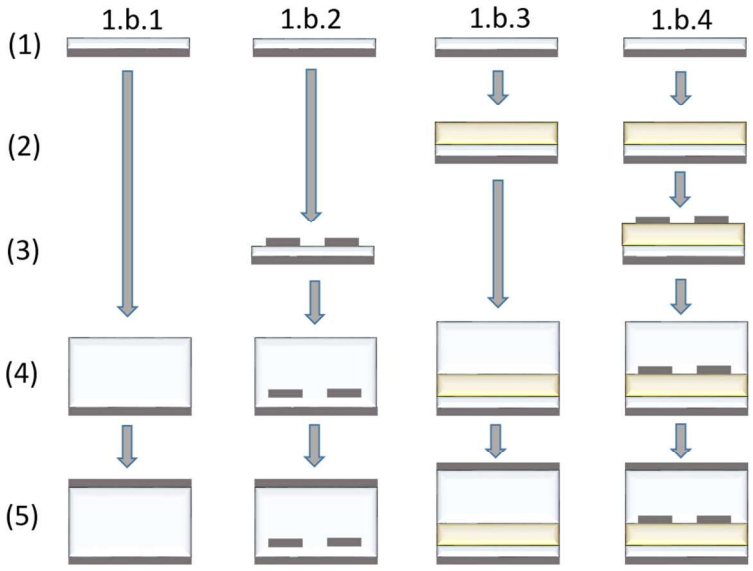

Figure S1. Process flow for fabrication of nano-cavities with 4 different geometries. (1) deposition of 25 nm thick Ag and 25 nm thick Al_2O_3. (2) depsition of 70 nm thick Ga:ZnO film. (3) e-beam lithography of metasurface and deposition of 2 nm-thick germanium as adhesion layer and 30 nm-thick Ag. (4) deposition of 800 nm-thick Al_2O_3 layer and Cl_2 RIE etching to achieve plannar surface with 205 nm-thick Al_2O_3 (5) deposition of 25 nm-thick Ag film for top mirror.

2. Design of Tunable Optical Nano-Cavity

To design the MIM metal cavity for the operation in transmission mode, the ratio between active (Ga:ZnO) and passive (Al_2O_3) component is critical for determining the modulation performance and the efficiency of the device. Figure S2 shows transmission spectrum of the nano-cavity with different filling factors of Ga:ZnO (FF= $L_{Ga:ZnO}/(L_{Ga:ZnO} + L_{Al_2O_3})$) for F-P resonance at the wavelength of 1.16 μm . The increase in the Ga:ZnO thickness decreases the transmission intensity at NIR resonances due to the intrinsic optical losses of Ga:ZnO arising from Drude damping of free carriers. Since the dynamic modulation of tunable nano-cavity is attributed from the index change of Ga:ZnO active layer under the optical pumping, it is required to determine the FF of Ga:ZnO to compromise modulation-losses tradeoff because the spectral modulation can be estimated by $2\Delta n L_{Ga:ZnO}$.

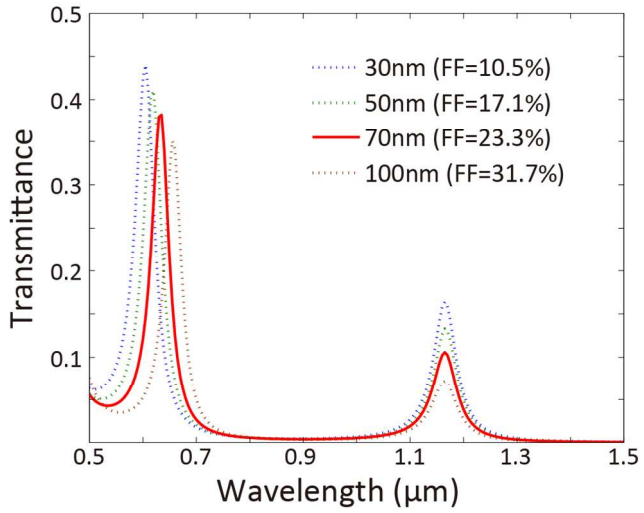

Figure S2. Simulation (dashed line) of transmission spectra of nano-cavity with 4 different filling factors (FF) of the Ga:ZnO active layer. The solid curve is the optimized spectrum which we used in the experiment.

3. Static Control of Cavity Resonance

Figure S3 shows the spectral transmission of nano-cavity embedded with metasurface only (Fig. S3a) and both metasurface and metal oxides (Fig. S3b). In any cases, the metasurface helps to

control the cavity resonance by adjusting the size of the width (W). As discussed in the manuscript, increasing the width of Ag metasurface can increase the phase shift inside the metasurface and the cavity resonance is red-shifted to satisfy the resonance condition of nano-cavity.

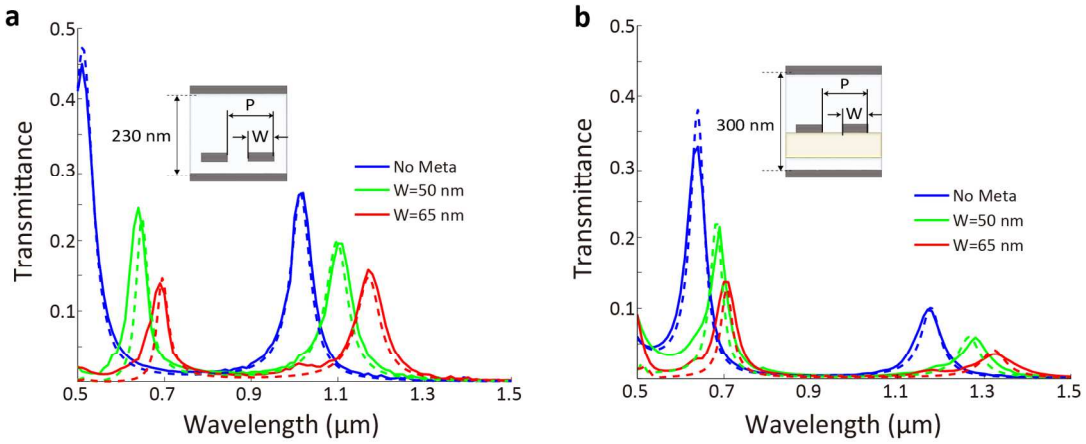

Figure S3. Experiment (solid line) and simulation (dashed line) of transmission spectra of nanocavity with different width of metasurface. **a)** nano-cavity with Ag metasurface. **b)** nano-cavity with both Ag metasurface and Ga:ZnO film. P and W is the perodicity and linewidth of Ag metasurface.

4.Two Temperature Model

The two-temperature model (TTM) successfully models the intraband dynamics of metal-like materials. This model describes the heat transfer of non-thermalized electron from the absorbed laser energy to the material. It is noted in previous studies that the small electron heat capacity in metal oxides enables large change in the electron temperature with relatively small laser fluence [1]. Excited electrons are relaxed by the electron phonon interaction, resulting in heat transfer from electron to lattice. The intraband dynamics of the Ga:ZnO film can be described as function of time and space:

$$C_e \frac{\partial T_e}{\partial t} = \frac{\partial}{\partial z}\left(k_e \frac{\partial T_e}{\partial z}\right) - g(T_e - T_l) + S(t) \qquad \text{(S1)}$$

$$C_l \frac{\partial T_l}{\partial t} = g(T_e - T_l) \quad \text{(S2)}$$

$$s(t) = \frac{4\ln(2)}{\pi} \frac{A}{t_p \delta_s} \phi \cdot \exp\left(\frac{-x}{\delta_s} - 4\ln(2)\left(\frac{t-2t_p}{t_p}\right)^2\right) \quad \text{(S3)}$$

where C_e is the heat capacity of electrons, $C_l$is the heat capacity of the lattice, k_e is the thermal conductivity, T_e is the temperature of the electrons, T_l is the lattice temperature, g is the electron-phonon coupling factor, and $s(t)$ is the source term given by Eq. (S3)[2]. Here, A is the absorption of Ga:ZnO thin film, ϕ is the excitation intensity, δ_s is the skin depth of the pump, and t_p is the pump duration. The large skin depth of Ga:ZnO permits us to approximate the spatial distribution of the electrons as a constant. The thermal conductivity (k_e) can be described as function of T_e

$$k_e = \frac{\pi^2 n_i k_b^2 T_e \mu_e}{3e} \quad \text{(S4)}$$

where n_i is the intrinsic carrier concentration, k_b is Boltzmann constant and μ_e is the electron mobility which we assumed to be temperature independent. In general, heat capacity of electrons (C_e) is a function of the electron temperature as described in Kittle[3]

$$C_e = \frac{\pi^2}{2} k_b \frac{T}{T_f} \quad \text{(S5)}$$

where $T_f = \frac{Ef}{K_b}$ is the Fermi temperature. The Fermi energy (E_f) of semiconductor can be is modeled using a Sommerfeld-Drude model which describes the chemical potential as function of temperature.

$$E_f(T_e) = E_f(0)\left[1 - \frac{\pi^2}{12}\left(\frac{T_e}{T_f}\right)^2\right] \quad \text{(S6)}$$

Lastly, g is calculated as $2\,C_e/\tau_{ep}$, where τ_{ep} is the electron-phonon collision time which is used to fit the decayed slope of absorption (transmission) transient as function of delay time between pump and probe. All constant parameters used in the calculation of TTM model are listed in Table S1.

Parameter	Value	Unit	Ref.
C_l	2.8×10^6	$J \cdot m^{-3} \cdot K^{-1}$	[4]
n_i	10^6	cm^{-3}	[5]
A	8	%	
t_p	100	fs	
δ_s	800	nm	
ϕ	9	$mJ \cdot cm^{-2}$	

4. Electronic Band Structure for Modelling of Carrier Distribution

In our previous study [6], doping effect on electron band structure and optical properties of 6 wt% doped Ga:ZnO was examined by first-principles density-functional thoery. Applying the lattice constant of Ga:ZnO characterized from x-ray diffraction (a = 3.296 Å, c = 5.294 Å), we calculate the available states per unit volume (cm^{-3}) per unit energy at room temperature. The lattice temperature is increased less than 3K at the intraband excitation, the lattice expansion is not under the consideration.

The non-parabolic conduction band dispersion is written as $\hbar^2k^2/2m^* = E + CE^2 = D(E)$, where m^* is the effective mass of electrons at the conduction band minimum and C is the non-parabolic constant. From conduction band dispersion relation, we can calculate the density of states per unit volume per unit $g_c(E,T)$ as below:

$$g_c(E,T) = m^*(T)^{3/2}\frac{\sqrt{2}}{\pi^2\hbar^3}D(E)' * D(E)^{1/2} \qquad \text{(S7)}$$

Since the g_c is proportional to the $m^{*3/2}$ as function of temperature, we can compute the $g_c(E)$ at different temperature by applying the change of m_n^* at different temperature based on the measured $m_e^*(300K) = 0.1911$ and $m_e^*(1891K) = 0.2263$.

References

[1] M. Z. Alam, I. De Leon, and R. W. Boyd, "Large optical nonlinearity of indium tin oxide in its epsilon-near-zero region," *Science* **352**, 795-797 (2016).

[2] T. Qiu and C. Tien, "Heat transfer mechanisms during short-pulse laser heating of metals," *Journal of heat transfer* **115**, 835-841 (1993).

[3] C. Kittel, *Introduction to solid state physics*: Wiley, 2005.

[4] H. Morkoç and Ü. Özgür, "Zinc Oxide," ed: Wiley-VCH Verlag GmbH & Co. KGaA, 2007.

[5] D. P. Norton, Y. Heo, M. Ivill, K. Ip, S. Pearton, M. F. Chisholm, and T. Steiner, "ZnO: growth, doping & processing," *Materials today* **7**, 34-40 (2004).

[6] J. Kim, G. V. Naik, A. V. Gavrilenko, K. Dondapati, V. I. Gavrilenko, S. Prokes, O. J. Glembocki, V. M. Shalaev, and A. Boltasseva, "Optical properties of gallium-doped zinc oxide—a low-loss plasmonic material: first-principles theory and experiment," *Physical Review X* **3**, 041037 (2013).